Ethanol-assisted *in situ* Stimulated graphene oxide as support for CuO/NiO nanoparticles

Manash J. Baruah,[†a] Eramoni Saikia,[†b] Nand Kishor Gour,[c] N Priyanshu Singh,[b] Bitupon Borthakur,[b] Uttam Mohan,[d] Arup Jyoti Das,[e] Rahul Kemprai,[f] Bikash K. Sarmah,[g] Rupjyoti Dutta,[h,i] Young-Bin Park,[j] Biraj Das[b]* and Mukesh Sharma[f]*

[a]*Department of Chemistry, D. C. B. Girls College, Jorhat, Assam, India, 785001*
[b]*Department of Chemistry, D. D. R. College, Chabua, Dibrugarh, Assam, India, 786184*
[c]*Department of Chemical Sciences, Tezpur University, Napaam, Tezpur, Assam, India, 784028,*
[d]*Department of Chemistry, D. H. S. K. College, Dibrugarh, Assam, India, 786001*
[e]*Department of Chemistry, Indian Institute of Technology, Kanpur, India, 208016*
[f]*Department of Chemistry, Suren Das College, Hajo, Kamrup, Assam, India, 781102*
[g]*Department of Chemistry, Sonari College, Sonari, Charaideo, Assam, India,785690*
[h]*CSIR-North East Institute of Science and Technology, Jorhat, Assam, India, 785006*
[i]*Academy of Scientific and Innovative Research (AcSIR), Ghaziabad, India, 201002*
[j]*Department of Mechanical Engineering, Ulsan National Institute of Science and Technology, UNIST-gil 50, Ulju-gun, Ulsan 44919, Republic of Korea*

[†] *Both the authors have equal contribution*

Material used:

Copper chloride ($CuCl_2$) and nickel chloride ($NiCl_2.6H_2O$) were purchased from E-Merck. Sodium hydroxide (NaOH) and Ethanol were brought from E-Merck. 4-nitrophenol and sodium borohydride ($NaBH_4$) were purchased from E-Merck.

Physical measurements

The Fourier-transform infrared (FTIR) spectroscopy spectrum was recorded in the mid-IR range of 450–4000 cm−1 using a Perkin-Elmer Frontier-MIR-FIR instrument. For solid samples, the FTIR measurements were conducted in DRIFT mode by grinding the samples with KBr. The Powder X-ray diffraction (PXRD) measurements were performed on a BRUKER AXS, D8 FOCUS instrument, focusing on low-angle measurements within the 2θ range of 10–80°. The Diffuse Reflectance Spectra (DRS) was obtained using a Hitachi U-

3400 spectrophotometer. Raman analyses were carried out using an EZ Raman-N (Enwave Optronics) spectrophotometer, utilizing a 150 mW, 785 nm laser through a 100× (0.3 N.A.) objective lens. The transmission electron microscopic (TEM) images as well as the energy dispersive X-ray (EDX) analyses were done on a JEM-2010 (JEOL) instrument equipped with a slow-scan CCD camera at an accelerating voltage of 200 kV. X-ray photoelectron spectroscopy (XPS) analysis was conducted on an ESCALAB Xi+ instrument manufactured by Thermo Fisher Scientific Pvt. Ltd., UK.

Computational Details:

Electronic structures of all species present in the proposed reaction mechanism are optimized using long-range corrected hybrid functional of Becke's 97 that incorporates dispersion correction i.e. ωB97XD functional [1] along with 6-311++G(d,p) basis set. We have further performed frequency calculations for all optimized species at the same level of theory. All these stable species were characterized by real and positive frequency values. All the theoretical calculation was performed by Gaussian 09 software [2].

Table S1 A comparative table outlining different synthetic routes for graphene oxide along with their preparation methods.

Synthetic Route	**Preparation Method**	**Reference(s)**
Hummers Method	Oxidation of graphite using $KMnO_4$, H_2SO_4, and $NaNO_3$	Hummers, W. S.; Offeman, R. E. J. Am. Chem. Soc. 1958, 80, 1339.
Staudenmaier Method	Oxidation of graphite using concentrated H_2SO_4, HNO_3, and $KClO_3$	Staudenmaier, L. Ber. Dtsch. Chem. Ges. 1898, 31, 1481.
Improved Hummers Method	Modified Hummers method using additional oxidizing agents or milder conditions	Marcano, D. C.; et al. ACS Nano 2010, 4, 4806.
Modified Staudenmaier Method	Variations of Staudenmaier method with different oxidizing agents or reaction conditions	Wang, G.; et al. J. Phys. Chem. C 2008, 112, 8192.
Hydrothermal Method	Oxidation of graphite under hydrothermal conditions	Park, S.; et al. Nano Lett. 2008, 8, 902.
Electrochemical Method	Electrochemical exfoliation of graphite in aqueous electrolytes	Ambrosi, A.; Pumera, M. Chem. Eur. J. 2016, 22, 2632.
Grinding Method	Metal precursors using Ethanol as template and heating	**This work**

Particle Size Distribution (PSD) Analysis of CuO/NiO/rGO from TEM images

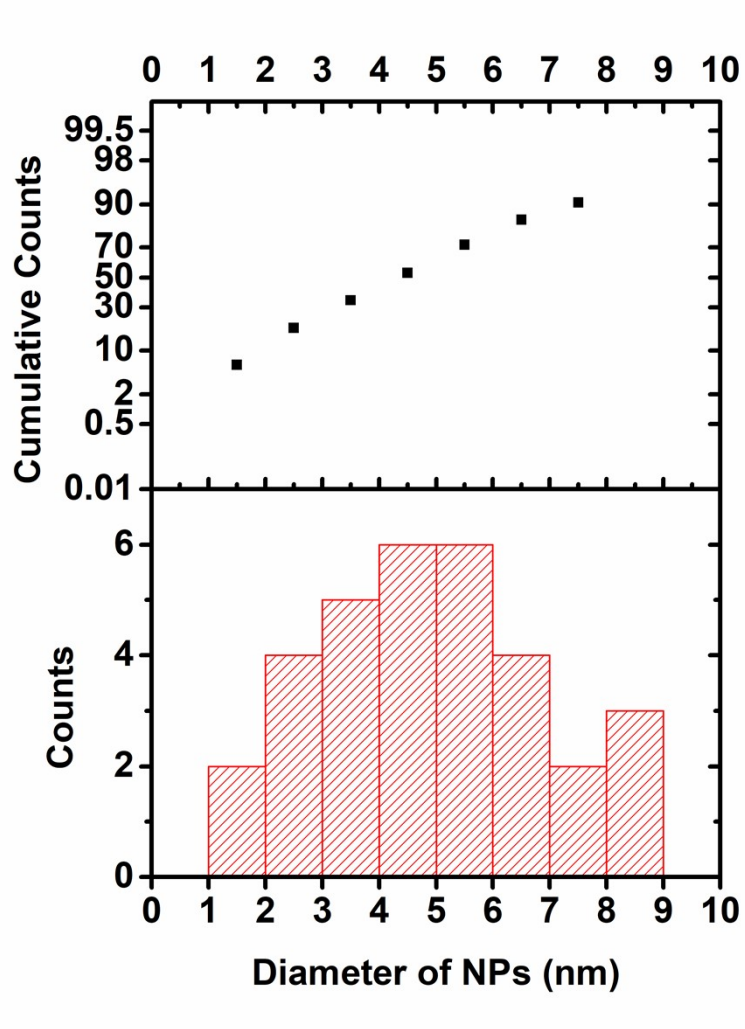

Fig. S1 PSD of CuO/NiO/rGO from the TEM images.

XPS Survey of CuO/NiO/rGO

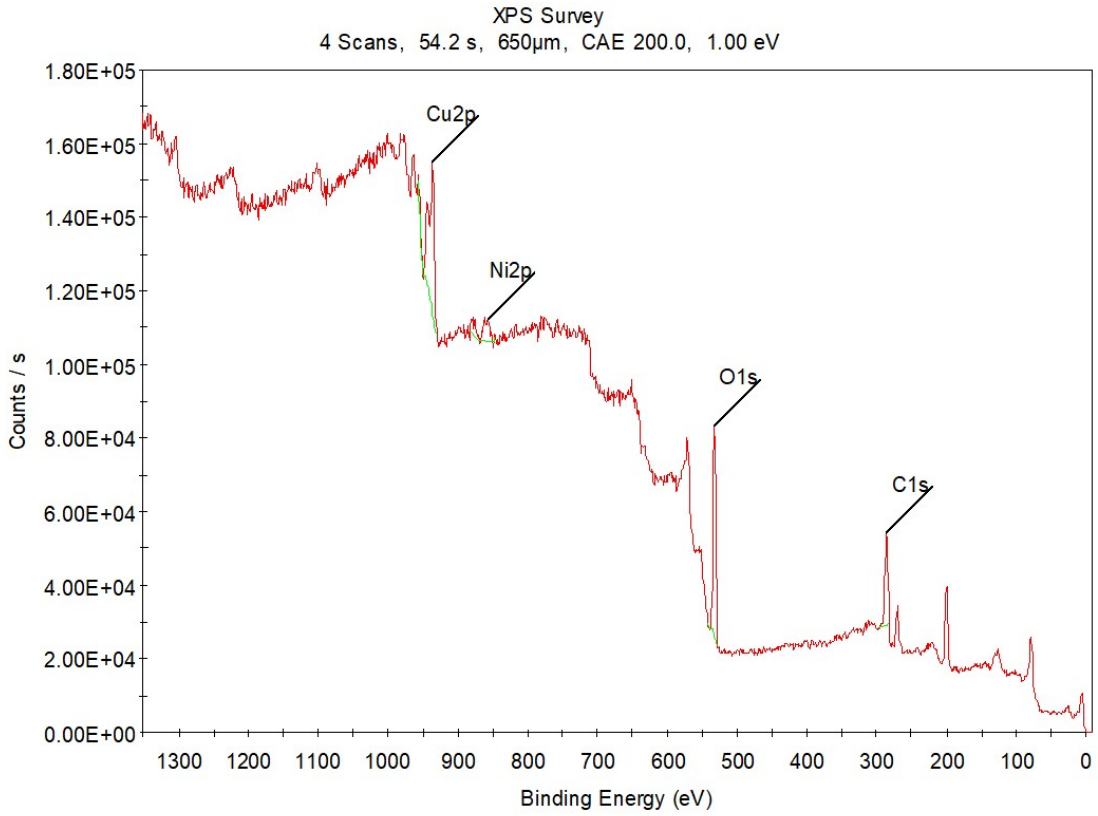

Fig. S2 Survey XPS of CuO/NiO/rGO.

Table S2 Atomic percentage of the elements from XPS data

Name	Start BE	Peak BE	End BE	Height CPS	FWHM eV	Area (P) CPS.eV	Area (N) TPP-2M	Atomic %
O1s	541	532.59	527	56998.1	4.45	269637.84	0.12	42.41
C1s	297	285.89	282	24490.56	4.17	117134.71	0.13	46.03
Ni2p	883	856.98	847	5687.75	3.9	92171.48	0.01	2.6
Cu2p	957	936.1	930	40783.99	5.77	372893.3	0.03	8.96

N_2-Adsorption Desorption Isotherm of CuO/NiO/rGO

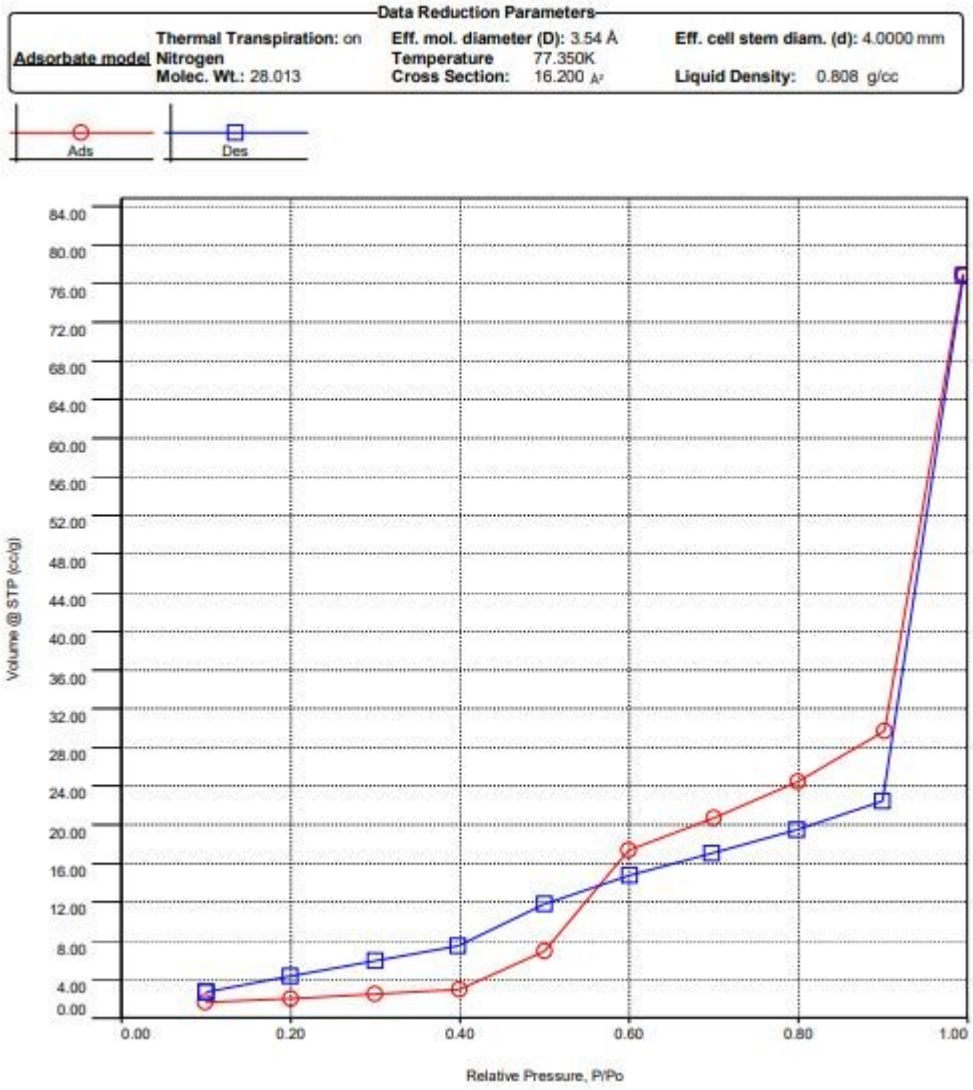

Fig. S3 N_2-adsorption desorption isotherm of CuO/NiO/rGO.

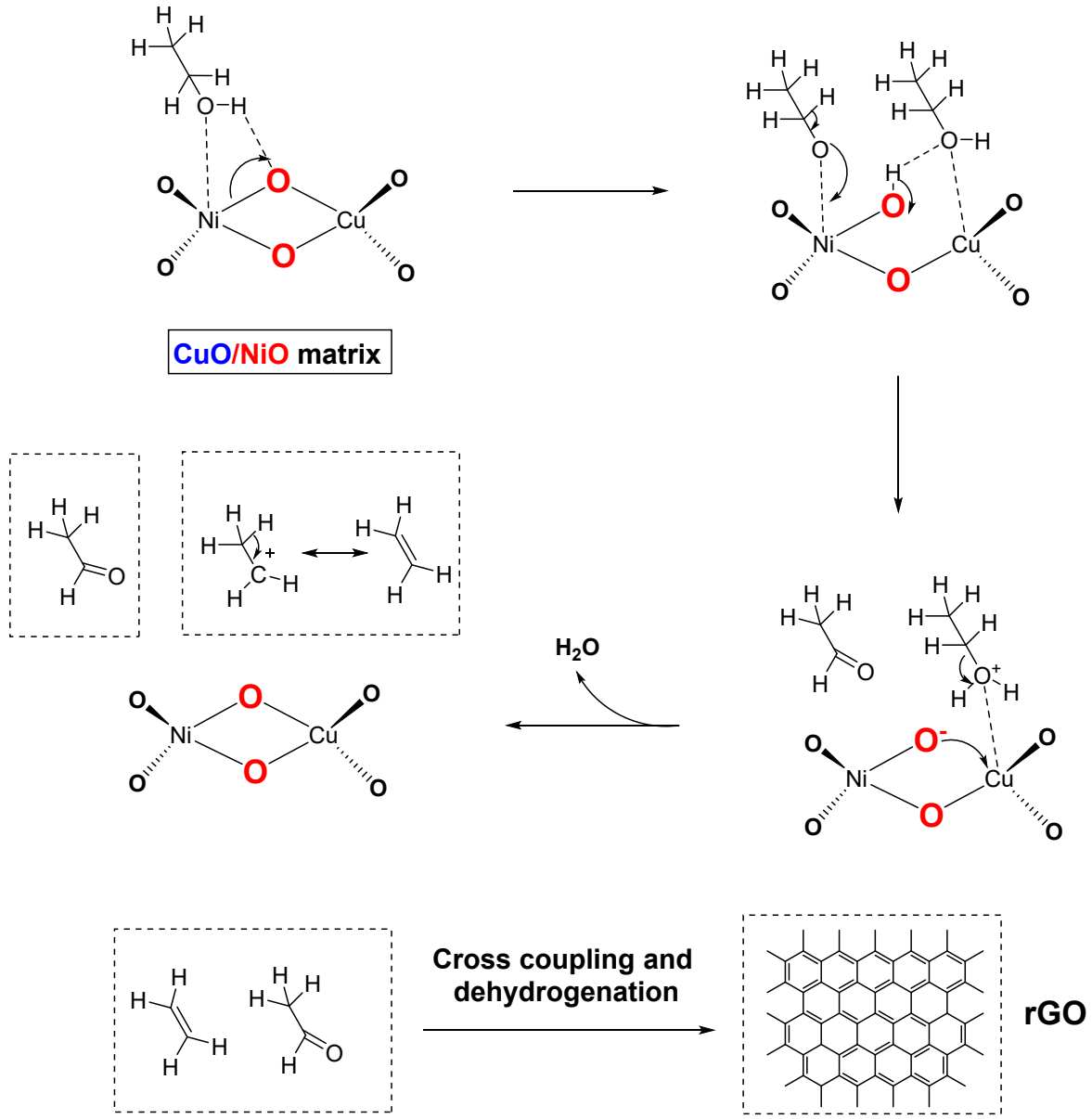

Scheme S1 Plausible mechanism for the formation of rGO using ethanol as a template.

Catalytic study of CuO/NiO/rGO in 4-nitrophenol reduction

To assess the catalytic performance of the synthesized nanomaterial, we conducted a reduction reaction involving the conversion of 4-NP to 4-AP using $NaBH_4$ as the reducing agent. The reaction was monitored at room temperature through UV-visible (UV-vis) spectrophotometry. As detailed in the experimental section, 3 mL of an aqueous 0.10 mM 4-NP solution was placed in a quartz cuvette for UV-vis analysis. The recorded absorption

spectrum showed a prominent peak at 402 nm, corresponding to the 4-nitrophenolate ion (Fig. S4a, black line). After adding 8 mg of CuO/NiO/rGO catalyst, a notable decrease in the intensity of this peak was observed over time, accompanied by the appearance of a new absorption peak at 296 nm (Fig. S4b, pink line) within 5 min. Initially, we recorded the UV-visible absorption spectrum of a 0.01 mM 4-NP solution, which exhibited a characteristic peak at 314 nm. Subsequently, we mixed 4 mL of the 4-NP solution with 100 µL of 0.01 mM $NaBH_4$, and UV-visible spectra were obtained using a standard quartz cuvette. Upon the addition of $NaBH_4$, the characteristic peak of 4-NP at 314 nm red-shifted to 402 nm, attributed to the deprotonation of the -OH group by $NaBH_4$, forming the corresponding 4-nitrophenolate ion. This red shift was also visually observable as the colour of the 4-NP solution changed from light yellow to dark yellow. Representative UV-visible absorption spectra for 4-nitrophenol and 4-nitrophenolate ion are depicted in Fig. S4a. To confirm the reduction of 4-NP to 4-AP after the addition of $NaBH_4$, the reaction mixture was stirred for 10 min, followed by recording a UV-visible absorption spectrum. However, no new peak corresponding to 4-AP was observed, indicating that the reduction had not occurred. Subsequently, the synthesized catalyst was introduced into the reaction mixture, and UV-visible spectra were recorded. A decrease in the intensity of the peak at 402 nm was noted, accompanied by a change in the solution's colour. With successive recordings of UV-visible spectra over time, a new peak emerged at 296 nm, characteristic of 4-AP formation (Fig. S4b). Notably, the absence of any other visible peaks and the presence of a clear isosbestic point between the absorption bands indicated the conversion of 4-NP to 4-AP without the formation of any byproducts. Furthermore, a blank experiment was conducted with a mixture of 4-NP and NPs only, where no reduction reaction was observed.

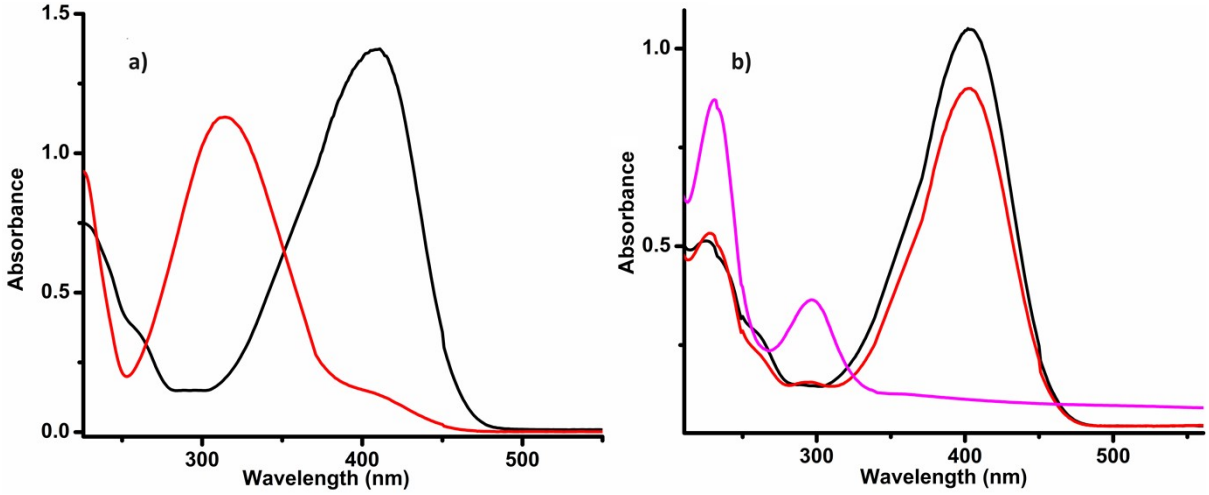

Fig. S4 a) UV-visible absorption spectra of 4-NP (red line) and 4-Nitrophenolate (black line) b) UV-visible absorption spectra of 4-AP (pink line) after the addition of CuO/NiO/rGO.

Optimization of catalyst activity

Literature studies have established that the catalytic activity of reduction reactions can be adjusted by altering the amount of catalyst used. Consequently, the effect of different catalyst dosages on the reduction of 4-NP was investigated using the synthesized CuO/NiO/rGO nanocomposite. The influence of varying amounts of the catalyst on the reduction of 4-NP was analysed, as shown in Fig. S5, which depicts the relationship between catalyst loading and the time required for the reaction to complete. Five distinct catalyst amounts (2, 4, 6, 8, and 10 mg) were tested while keeping other reaction conditions constant. The results clearly show that increasing the catalyst dosage significantly reduces the reaction time, likely due to the increased availability of active catalytic sites.

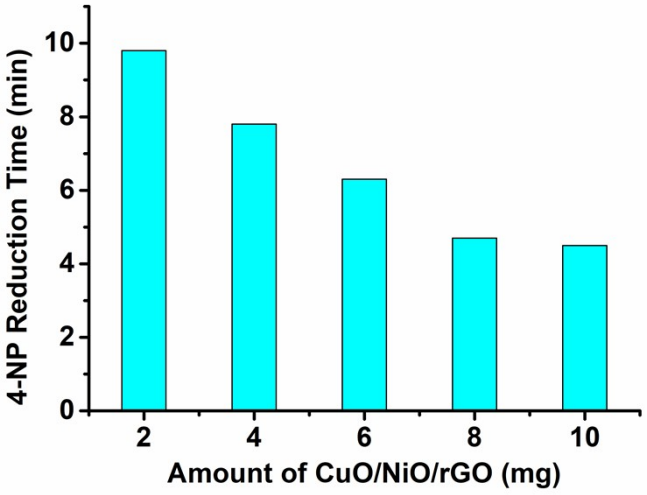

Fig. S5 Optimization of the amount of CuO/NiO/rGO for 4-NP reduction.

Table S3 Comparative study of some reported Cu-oxide/Ni-oxide bimetallic catalysts for 4-NP reduction.

Sl. No.	**Catalyst**	**Reducing Agent**	**Synthesis Process**	**Time (min)**	**Reference**
1	CuNi nanocubes	$NaBH_4$	Colloidal synthesis	6	Li, et al. *MRS Advances*, 2020, 5(27-28), 1491-1496.
2	CuNi NPs	$NaBH_4$	Polyol method	20	Sanyal et al. *SN Applied Sciences*, 2019, 1, 1-10.
3	NiCu nanocatalyst	$NaBH_4$	Laser synthesis	7	*Haladu et al. Journal of Molecular Structure*, 2024, 139930.
4	NiCu/C@SiO_2	H_2	Impregnation method	108	*Sheng et al Materials Advances. 2021,* **2***(20), 6722-30*
5	$Ni_{1.75}Cu$	$NaBH_4$	Reduction process	8.3	Avalos-Ballester et al. *ACS Omega 2024, 9, 36, 37981–37994*
6	CuO/NiO/rGO	$NaBH_4$	Grinding/Thermal	5	This work

References:

1. Y. S. Lin, G.-D. Li, S. P. Mao and J. D. Chai, *J. Chem. Theory Comput.*, 2013, **9**, 263–272.
2. M. J. Frisch, G. W. Trucks, H. B. Schlegel, G. E. Scuseria, M. A. Robb, J. R. Cheeseman, G. Scalmani, V. Barone, B. Mennucci, G. A. Petersson *et al.*, *Gaussian 09, Revision D.01*, Gaussian, Inc., Wallingford, CT, 2009.